Concurrent enteric helminth infection modulates inflammation and gastric immune responses and reduces helicobacter-induced gastric atrophy

JAMES G. FOX[1], PAUL BECK[3], CHARLES A. DANGLER[1], MARK T. WHARY[1], TIMOTHY C. WANG[3], HAI NING SHI[2] & CATHRYN NAGLER-ANDERSON[2]

[1]*Division of Comparative Medicine, Massachusetts Institute of Technology Cambridge, Massachusetts, 02139, USA*
[2]*Mucosal Immunology Laboratory, Pediatric Gastroenterology and* [3]*Gastroenterology Unit Department of Medicine, Massachusetts General Hospital, Boston, Massachusetts 02114, USA*
Address correspondence to J.G.F.; email: jgfox@mit.edu

***Helicobacter pylori* is causally associated with gastritis and gastric cancer. Some developing countries with a high prevalence of infection have high gastric cancer rates, whereas in others, these rates are low. The progression of helicobacter-induced gastritis and gastric atrophy mediated by type 1 T-helper cells may be modulated by concurrent parasitic infection. Here, in mice with concurrent helminth infection, helicobacter-associated gastric atrophy was reduced considerably despite chronic inflammation and high helicobacter colonization. This correlated with a substantial reduction in mRNA for cytokines and chemokines associated with a gastric inflammatory response of type 1 T-helper cells. Thus, concurrent enteric helminth infection can attenuate gastric atrophy, a premalignant lesion.**

Helicobacter pylori is now considered to be the most prevalent infectious disease known to occur in humans; about 50% of the human population is estimated to be infected[1]. *H. pylori* causes persistent gastritis and is directly linked to the development of peptic ulcer disease as well as gastric adenocarcinoma and mucosa-associated lymphoma of the stomach[2]. Fortunately, only a small percentage of the population will develop serious disease due to *H. pylori* infection. Why some individuals develop disease and others do not is unknown; host and environmental factors as well as the virulence properties of particular strains of *H. pylori* probably influence disease outcome in infected individuals. Individuals living in countries with low socioeconomic conditions have high prevalence rates of *H. pylori* acquired at an early age[3]. Some of these countries have high rates of gastric cancer (such as Colombia and Peru), whereas some African countries with equally high prevalence rates of *H. pylori* have much lower gastric cancer. This paradox has been referred to as the 'African enigma'[4]. Several theories have been advanced to provide a rationale for this observation; diet and relatively short life span have been suggested as contributing factors.

Another possibility is the influence of concurrent infection with other pathogens on the immune response to *H. pylori*. $CD4^+$ T cells can be divided into two functional subsets, type 1 and type 2 T-helper cells (Th1 and Th2 cells), which are defined by their pattern of cytokine secretion. Th1 cells produce interleukin (IL)-2 and interferon (IFN)-γ and promote cell-mediated immune responses, including delayed type hypersensitivity. Th2 cells secret IL-4, IL-5, IL-6 and IL-10 and induce B-cell activation and differentiation. The cytokines secreted by each of these subsets regulate those produced by the other subset. Indeed, recent evidence has indicated that the immune response to a variety of infectious agents is accompanied by a preferential expansion of one subset with a concomitant downregulation of the other[5]. Many intracellular bacteria, protozoa and fungi induce Th1 responses, whereas extracellular pathogens, particularly helminthic parasites, drive polarized Th2 responses. The degree of polarization varies, depending on the nature of the infection and its persistence. The immune response elicited by both infection with *H. pylori* in humans and infection with *H. felis* in mice has been described as being Th1-like because inflammatory cells in the infected hosts produce higher amounts of IFN-γ than IL-4 (refs. 6,7). Research in murine models has shown that host T-cell response is the essential mediator of helicobacter-associated gastric pathology[8,9]. Given that concurrent infections with Th2-inducing helminths are also endemic in developing countries with a high prevalence of *H. pylori* infection, helminth infections might modulate a pro-inflammatory Th1 response to gastric helicobacter infection towards a less-injurious Th2 response. Thus, we examined the progression of helicobacter gastritis and the development of gastric atrophy in C57BL/6 mice co-infected with *H. felis* and *Heligmosomoides polygyrus*, a natural murine nematode parasite with a strictly enteric life cycle[10].

Helminth infection reduces helicobacter gastritis

Mice infected with *H. felis* for 8 weeks had moderate-to-severe corpus gastritis, which extended throughout the corpus mucosa to the antrum. Inflammation was characterized by a chronic inflammatory cell infiltrate composed mostly of lymphocytes, which formed discrete foci or follicles in the deep mucosa and submucosa (Fig. 1*a*). Mild granulocytic infiltration was also present in the gastric corpus. Alterations in mucosal epithelium were extensive and emanated from the proximal corpus, adjacent to the squamocolumnar junction. Hyperplasia of the gastric pit epithelium was profound, along with mucous metaplasia and moderate parietal cell loss.

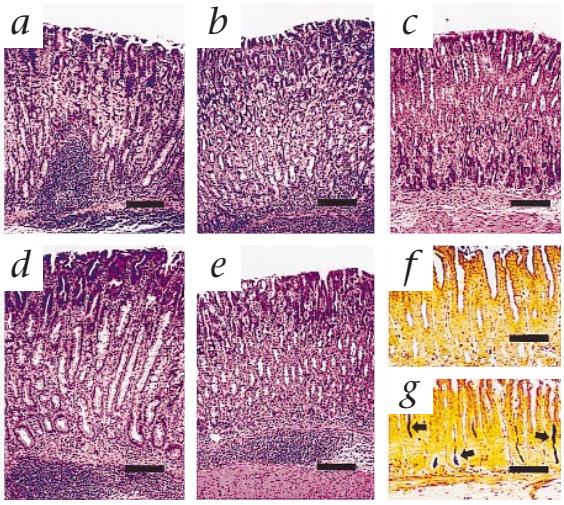

Fig. 1 Effect of concurrent enteric *H. polygyrus* infection on *H. felis*-associated gastritis in mice. ***a***, At 8 weeks after infection with *H. felis* only, the corpus mucosa has moderate hyperplasia and extensive loss of parietal cells, associated with intramucosal and submucosal lymphoid infiltration. ***b***, At 8 weeks after infection, concurrent *H. polygyrus* infection is associated with substantial retention of parietal cells despite considerable local inflammation. At this time, granulocytic infiltration is much greater in mice with concurrent *H. polygyrus* infection. ***c***, In contrast to the obvious patterns of *H. felis*-induced gastritis, *H. polygyrus* alone has no effect on the histology of the corpus mucosa. ***d***, At 16 weeks after infection, *H. felis* infection progresses to considerable atrophic corpus gastritis, characterized by mucosal epithelial hyperplasia, mucous cell hypertrophy and metaplasia, and effacement of the parietal cell zone. ***e***, At 16 weeks after infection, atrophic gastritis is substantially decreased in mice co-infected with *H. polygyrus*. There is retention of parietal cell numbers, compared with that in infection with *H. felis* alone. ***f***, Colonization of the antral mucosa is typically inapparent in Warthin-Starry silver-stained sections from the group infected with *H. felis* only. ***g***, At 16 weeks after infection, the antral mucosa is densely colonized (arrows) by large argyrophilic, spiral bacteria resembling *H. felis* in mice with concurrent *H. polygyrus* infection. Scale bars represent 150 μm (*a*–*e*) and 75 μm (*f* and *g*).

In contrast, mice infected with *H. felis* for 8 weeks after pre-infection with *H. polygyrus* had limited corpus gastritis. There was a significant decrease in scores for chronic inflammation in the corpus submucosa ($P < 0.05$). Mucosal lymphocytic infiltration also tended to be diminished. Granulocytic infiltration in the gastric corpus was moderate to severe and significantly more ($P < 0.05$) than that seen with infection with *H. felis* alone (Figs. 1*b* and 2*a*). Mucosal epithelium alterations, as described for infection with *H. felis* alone, were present; however, the extent and severity were less, and sometimes spared the proximal corpus. Parietal cell density was well-maintained despite local inflammation; this differed significantly from that in mice infected solely with *H. felis* ($P < 0.05$) (Figs. 1*b* and 2*a*). Antral colonization by *H. felis* was greater in the mice concurrently infected with *H. polygyrus*. Gastric mucosal alterations and inflammation were not substantial in mice without *H. felis* infections, regardless of the status of infection with *H. polygyrus*, at either 8 or 16 weeks after infection (Fig. 1*c*).

Infection with *H. felis* alone at 16 weeks after infection was associated with considerable diffuse atrophy of the glandular epithelium of the corpus mucosa, resulting in extensive replacement of parietal cells by hyperplastic mucous epithelium (Fig. 1*d*). There were submucosal foci of invasive hyperplastic mucous epithelium in two mice. The most intense inflammation was centered on the corpus region, composed of a moderate-to-substantial lymphoplasmacytic infiltrate accompanied by a moderate granulocytic component. Prominent lymphoid aggregates, although frequent in the submucosa, were comparatively rare in the mucosa.

Co-infection with *H. polygyrus* and *H. felis* was associated with distinct gastric lesions. Mucosal hyperplasia, parietal cell loss and mucous metaplasia were all significantly less than in the group infected with *H. felis* ($P < 0.05$) (Fig. 2*b*). Although there was hyperplasia of the gastric pit epithelium, there was only a mild loss of parietal cell mass of the corpus mucosa in four of five mice (Fig. 1*e*). Inflammation in the corpus region was composed of lymphoplasmacytic and granulocytic infiltrates, similar to that seen in the group infected with *H. felis*. Intramucosal lymphoid aggregates were frequent.

Although inflammatory scores were high for both groups initially decreased, although active (granulocytic) infiltrates are substantially increased. All three categories of mucosal alteration in the corpus show a trend towards less severity in mice concurrently infected with *H. polygyrus*; relative sparing of the parietal cells is statistically significant in mice concurrently infected with *H. polygyrus*. ***b***, After 16 weeks infection with *H. felis*, mucosal alterations are substantially decreased in mice co-infected with *H. polygyrus*. However, bacterial colonization is typically high, and is much higher than that in mice infected solely with *H. felis*.

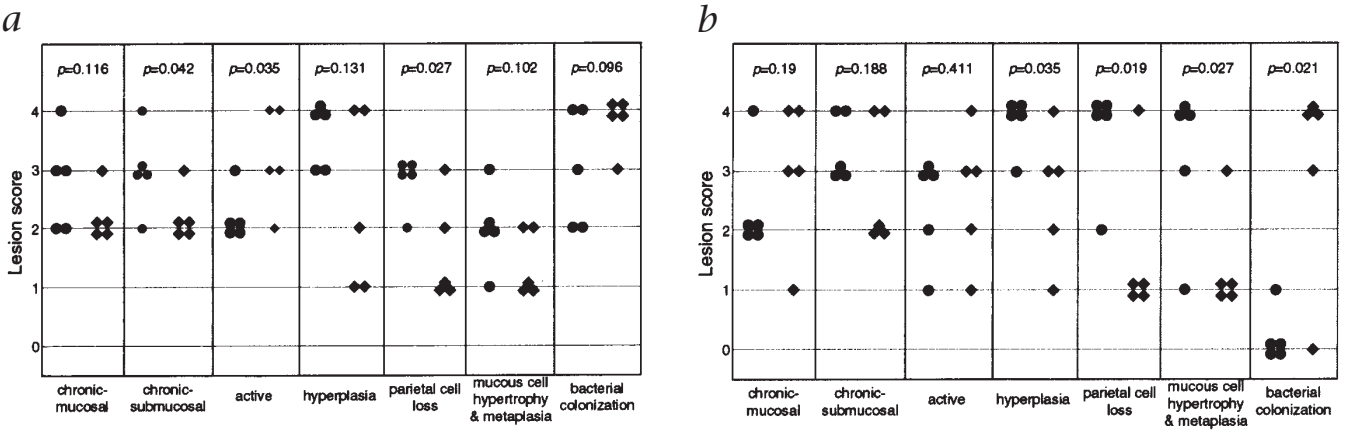

Fig. 2 Effect of *H. polygyrus* co-infection on the histopathologic gastric changes induced by infection with *H. felis*. Columns 1–3, inflammatory changes in the gastric corpus region; columns 4–6, mucosal epithelial alterations; column 7, densities of bacterial colonization in the antral mucosa. Cirlces, *H. felis*; diamonds, *H. felis* plus *H. polygyrus*; number of symbols indicates number of mice achieving that score. ***a***, After 8 weeks of infection with *H. felis*, in association with co-infection with *H. polygyrus*, chronic (lymphohistiocytic and plasmacytic) infiltrates in the submucosa are substan-

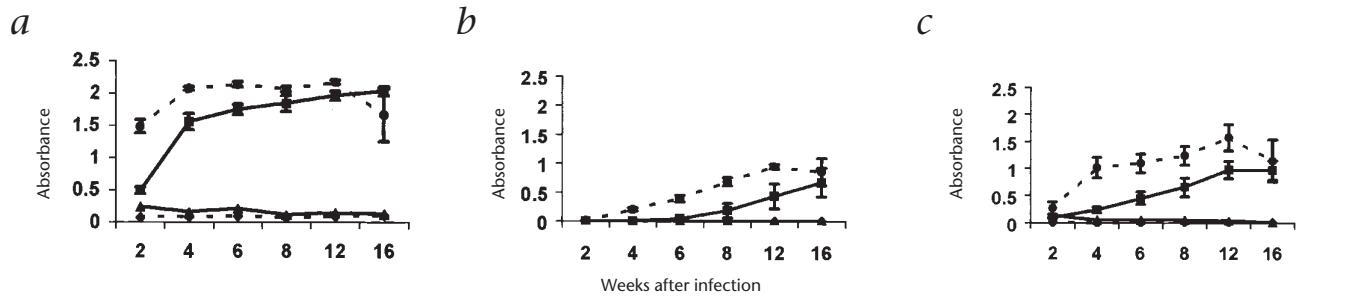

Fig 3 Helminth infection alters *H. felis*-specific IgG1 and IgG2a. Serum levels of IgG were measured by ELISA in control mice (◆) and mice infected with either *H. polygyrus* (▲) or *H. felis* (●) or co-infected with both (■). ***a***, Mice infected with *H. felis* alone develop a greater IgG response through 6 weeks after infection ($P < 0.0002$), after which time IgG levels plateau and are similar ($P = 0.063$ and higher) in mice infected with *H. felis* alone and those co-infected with *H. felis* and *H. polygyrus*. ***b*** and ***c***, Similar results are obtained in a comparison of the *H. felis*-specific IgG2a (*b*) and IgG1 (*c*) responses in mice infected with *H. felis* alone and mice co-infected mice ($P < 0.03$ and 0.04, respectively, through 12 weeks after infection). The Ig2a (Th1) response is inhibited more than the IgG1 (Th2) response at 4 and 6 weeks after infection ($P < 0.02$). Error bars represent 1 standard error of the mean.

fected with *H. felis*, along with differences in the development of gastric atrophy, there was a salient difference in colonization by *H. felis*. At 16 weeks after infection, colonization by *H. felis* was typically not perceptible in mice infected with *H. felis* alone (Fig. 1*f*). Gastric colonization by *H. felis* was significantly greater in the group co-infected with *H. polygyrus* ($P < 0.05$; Fig. 2*b*), and was characterized by typically dense colonization in the antrum and extension into the corpus mucosa (Fig. 1*g*).

At 16 weeks after infection, one dually infected mouse had a diffuse glandular atrophy and mucosal hyperplasia, resembling that of the group infected with *H. felis*. Colonization by *H. felis* also was not visible. Although this mouse had an immunoglobulin profile consistent with that of the group infected with *H. polygyrus* and had high levels of expression of IL-4, its levels of IFN-γ and TNF-α transcripts were uncharacteristically high for this group, again more closely resembling those of the group infected with *H. felis*. Similarly, 16 weeks after infection with *H. felis*, one mouse had less expression of IFN-γ and TNF-α than did its cohorts. This variation corresponded to limited development of gastric atrophy, typical of the dually infected group.

Helminth infection alters *H. felis*-specific serum antibody

Levels of *H. felis*-specific serum IgG from mice infected with *H. felis* or co-infected with *H. felis* and *H. polygyrus* were significantly higher than control levels by 2 weeks after infection ($P < 0.0001$; Fig. 3*a*). Compared with mice co-infected with *H. felis* and *H. polygyrus*, mice infected with *H. felis* developed a greater IgG response through 6 weeks after infection ($P < 0.0002$). At 8 weeks after infection, the IgG response of these two groups of mice infected with *H. felis* were similar and plateaued for the remaining time. At all times between 4 and 16 weeks after infection with *H. felis*, the serum IgG2a and IgG1 responses to *H. felis* from mice co-infected with *H. polygyrus* and *H. felis* were less than the responses of mice infected with *H. felis* alone (Fig. 3*b* and *c*). However, the Th1-dependent (IgG2a) serum antibody response to *H. felis* antigens was downregulated more than the Th2-dependent (IgG1) antibody response, particularly at 4 and 6 weeks after infection. IgA responses are also dependent on Th2 cytokines. Fecal extracts collected from mice infected with *H. felis* contained high levels of IgA antibody against *H. felis* at 8 and 16 weeks after infection At 8 weeks after infection, there was a trend towards higher IgA levels in mice infected with *H. felis* than in co-infected mice ($P = 0.055$). At 16 weeks after infection, there was no difference in the IgA response to *H. felis* between mice infected with *H. felis* alone and those co-infected with *H. polygyrus* (data not shown).

Helminth-induced IgE and IgG1 are unaltered by *H. felis*

Total serum IgE and IgG1 levels were increased in mice infected with *H. polygyrus* (Fig. 4), as would be expected for a polarized Th2 immune response[10]. To ascertain whether subsequent helicobacter infection altered this helminth-induced Th2 response, we determined total IgE and IgG1 serum levels at 8 and 16 weeks after infection. IgE was only detectable in the sera of mice infected with *H. polygyrus*, and the levels were similar with and without co-infection with *H. felis* (Fig. 4). By 16 weeks after infection, IgE levels had begun to decrease. Non-infected control mice had mean total serum IgG1 levels of 331 ± 34 μg/ml and 254 ± 14 μg/ml at 8 and 16 weeks after infection, respectively, similar to levels in mice infected with *H. felis* (360 ± 28 and 267 ± 46 μg/ml, respectively) (Fig. 4). At 8 and 16 weeks after infection, total IgG1 levels were almost 200% higher in mice infected with *H. polygyrus* (541 ± 27 and 512 ± 20 μg/ml, respectively) and were not altered by co-infection with

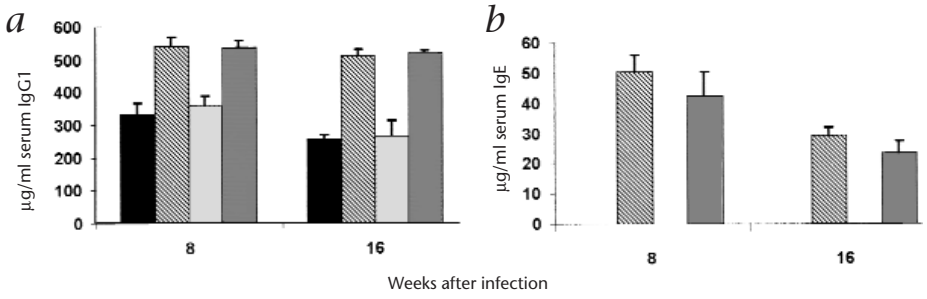

Fig. 4 Subsequent helicobacter infection does not alter the helminth-induced Th2 response. As evidence of a Th2 response to *H. polygyrus*, serum levels of IgG1 (***a***) and IgE (***b***) are increased in parasitized mice. Levels in co-infected mice (■) are similar to those in mice infected with *H. polygyrus* alone (▨). ■, control mice; ■, mice infected with *H. felis* alone. Error bars represent 1 standard error of the mean.

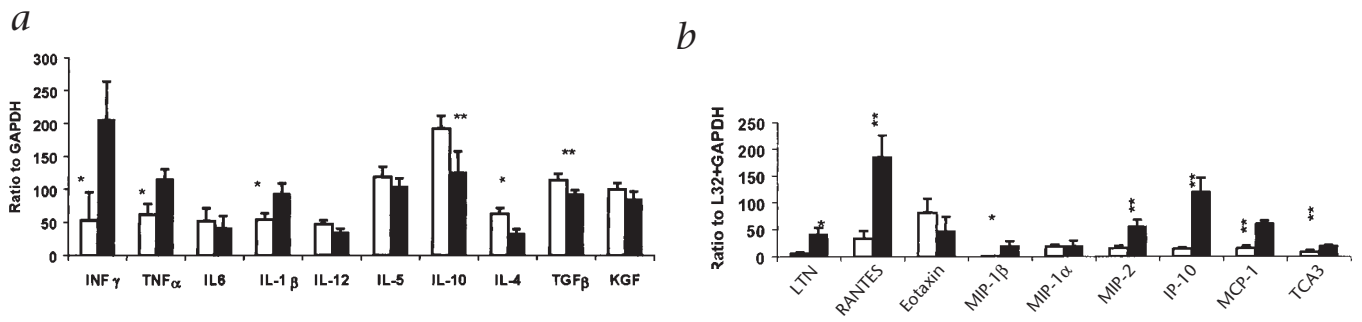

Fig. 5 Inflammatory cytokines and chemokines are decreased in co-infected mice. ***a***, mRNA for cytokine gene expression in gastric biopsies at 16 weeks after infection with *H. felis*, assessed by RT–PCR. Co-infected mice (open bars) have lower levels of mRNA for the Th1 cytokines TNF-α, IFN-γ and IL-1β than do mice infected with *H. felis* alone (filled bars). Furthermore, co-infected mice have significantly higher levels of mRNA for the Th2 cytokines IL-4, Il-10 and TGF-β than do mice infected with *H. felis* alone. Error bars represent 1 standard error of the mean. *, $P < 0.03$; **, $P < 0.04$. ***b***, Chemokine gene expression, measured by ribonuclease protection assay as mRNA expressed in gastric biopsies 16 weeks after infection with *H. felis*. mRNA for the chemokines IP-10, MIP-1β and RANTES is increased in mice infected with *H. felis* alone (filled bars). Expression of these chemokines is downregulated by concurrent helminth infection (open bars); expression of the Th2 associated chemokine eotaxin is slightly increased. Error bars represent 1 standard error of the mean. *, $P < 0.05$; **, $P < 0.02$.

H. felis (537 ± 23 and 518 ± 11 μg/ml, respectively). Few viable nematodes were detectable in the intestinal lumens of mice infected with *H. polygyrus* (with or without co-infection) at necropsy at 16 weeks after infection (data not shown).

Th1 cytokine chemokine mRNA decreases in co-infection

We determined the gastric cytokine and chemokine mRNA expression in all mice 16 weeks after infection with *H. felis* or co-infection with *H. felis* and *H. polygyrus*, by semi-quantitative RT–PCR (for cytokines) or ribonuclease protection assay (for chemokines), using GAPDH and L32 as internal controls. Co-infected mice had significantly ($P < 0.03$) lower levels of mRNA for the Th1 cytokines IFN-γ, TNF-α and IL-1β than did mice infected with *H. felis* alone (Fig. 5*a*). Furthermore, co-infected mice had significantly ($P < 0.01$-0.04) higher levels of mRNA for the Th2 cytokines IL-4, IL-10 and transforming growth factor (TGF)-β than did mice infected with *H. felis* alone. There were no differences in the levels of expression of IL-5, IL-6, IL-12 and keratinocyte growth factor in mice infected with *H. felis* with or without co-infection with *H. polygyrus*.

Chemokines are central in the recruitment of activated T cells into sites of inflammation. Th1 and Th2 cells preferentially migrate in response to certain chemotactic stimuli; differential chemokine receptor expression, therefore, seems to govern the 'homing' of Th1 and Th2 cells[11–14]. Th1 inflammatory responses are characterized by the expression of the chemokine receptors CXCR3, which bind the chemokine interferon-inducible protein (IP)-10, and CCR5, which binds RANTES (regulated upon activation, normal T-cell expressed and secreted), macrophage inflammatory protein (MIP)-1α and MIP-1β. As expected for a Th1 inflammatory response, levels of mRNA for the chemokines IP-10, RANTES and MIP-1β were increased in the stomachs of mice infected with *H. felis* ($P < 0.02$–0.05; Fig. 5*b*). The expression of mRNA for each of these chemokines was decreased considerably by concurrent helminth infection. Expression of the Th2-associated chemokine eotaxin was also slightly increased.

Discussion

Helicobacter infection in both humans and C57BL/6 mice is associated with a Th1-like immune response[6,7,15]. In C57BL/6 mice, chronic helicobacter infection is associated with considerable gastric inflammation and corpus atrophy, which is considered a premalignant gastric lesion. In contrast, BALB/c mice respond to the gastric helicobacter with a Th2-like response and develop minimal gastritis despite the presence of dense colonization with *H. felis*[16]. Furthermore, studies in recombination activation gene-1$^{-/-}$ mice, T-cell receptor-β$\delta^{-/-}$ mice deficient in T cells, and severe combined immunodeficiency mice (all on a C57BL/6 background) have shown that the T-cell response to *H. felis* and/or *H. pylori* is an essential element in the initial pathway of gastritis to corpus atrophy[8,9]. Because infection with *H. polygyrus* elicits a polarized Th2 response, we determined whether co-infection of *H. felis* and *H. polygyrus* would have a modulating effect on gastric mucosal inflammation of dually infected mice compared with that in mice infected with either the parasite or helicobacter alone. We expected that parasite-induced anti-inflammatory Th2 cytokines (such as IL-4 and IL-10) would antagonize pro-inflammatory Th1 responses induced by gastric helicobacter infection. This was supported by mRNA analysis of both cytokines (Fig. 5*a*) and chemokines (Fig. 5*b*) in the gastric mucosa, as well as by the *H. felis*-specific humoral responses in mice co-infected with *H. polygyrus* and *H. felis* (Fig. 3). Co-infected mice had significantly lower gastric levels of mRNA for IFN-γ, TNF-α and IL-1β than did mice infected with *H. felis* alone. Moreover, mice infected with *H. felis* and co-infected with *H. polygyrus* responded with significantly more gene expression for the Th2 cytokines IL-4, IL-10 and TGF-β than did mice infected with *H. felis* alone. IFN-γ production at sites of inflammation can induce chemokine gene expression. The significantly decreased gene expression for the chemokines IP-10, monocyte chemotactic peptide-1 and RANTES, therefore, may be related to the decreased local IFN-γ mRNA expression in the co-infected mice[17-19]. Downregulation of chemokine expression may block the migration of inflammatory Th1 cells into the stomach, ameliorating the helicobacter-associated gastric histopathology.

As expected, mice infected with *H. felis* had moderate-to-severe corpus gastritis at 8 weeks after infection, which progressed at 16 weeks after infection to a profound diffuse atrophy of the corpus glandular mucosal epithelium with compensatory replacement by a proliferative, metaplastic mucous metaplasia. This metaplastic epithelium was characterized by a transition from a neutral mucin secretion to an intestinal mucin phenotype, acid sialomucin,

which can be demonstrated histochemically with and Alcian blue stain at a pH of 2.5 (not shown). The expansion of this mucous epithelium with replacement of the normal corpus glands, and its histochemical staining pattern have been described in susceptible mouse strains infected with *H. felis*[20,21]. There was also submucosal invasive hyperplastic epithelium in mice infected with *H. felis*, which is derived from the metaplastic mucous epithelium[22]. This invasive behavior has also been described in mice with severe *H. felis*-induced gastritis[20]. Inflammation was mainly restricted to the corpus and lymphoid aggregates were restricted to the submucosa. In contrast, co-infected mice at 8 weeks after infection had a substantially diminished mononuclear inflammatory response in glandular epithelium of the stomach, whereas their granulocytic response was significantly higher. The glandular corpus was preserved without loss of chief and parietal cells. Unlike mice infected with *H. felis* alone, the co-infected mice remained heavily colonized with *H. felis*. This is analogous to mice infected with *H. felis* that respond to the infection with a Th2-like response[16], and is also consistent with findings of the higher gastric colonization by *H. pylori* in IFN-$\gamma^{-/-}$ mice than in C57BL/6 wild-type mice[15]. Thus, the lower levels of gene expression for gastric IFN-γ in the co-infected mice may provide an explanation for higher colonization of *H. felis* in these mice. Also supportive of our findings is the observation that, despite a chronic, 15-month infection with *H. pylori*, the IFN-$\gamma^{-/-}$ mice have minimal gastritis, compared with the severe inflammation in the stomachs of C57BL/6 mice infected with *H. pylori*[15]. Furthermore, IFN-γ levels measured by RT–PCR are a useful predictor of degree of gastritis in C57/BL6 mice infected with *H. pylori*[23].

Two outlying data points at 16 weeks after infection indicate there are other variables that determine the balance of Th1 and Th2 responses and may offset the substantial influence of the enteric helminth infection. At 16 weeks after infection, one mouse from the dually infected group developed considerable atrophic gastritis and elimination of discernible colonization by *H. felis*, indistinguishable from results in mice infected with *H. felis* only. Nonetheless, this mouse had high concentrations of IgE and IgG1, consistent with those of the dually infected group. This mouse had uniquely high expression levels of IL-4 and IL-10 as well as IFN-γ and TNF-α, indicating the Th2-associated cytokines IL-4 and IL-10 are not solely predictive of the downregulation of IFN-γ and TNF-α. A second mouse infected with *H. felis* only manifested a response to *H. felis* somewhat atypical for its group, although its deviation was less substantial than that of the former mouse. In this latter mouse, atrophic gastritis was not as fulminant as in its cohorts and was associated with low expression of both IFN-γ and TNF-α. Expression of IL-4 was also low in this mouse, and expression of IL-10 was intermediate.

A recent report using a similar co-infection strategy examined the influence of an ongoing helminth-induced Th2 response on an infection with the Th1-inducing protozoan parasite *Toxoplasma gondii*, and described a very different outcome[24]. As in our model, the polarized Th2 response induced by an ongoing infection with *Schistosoma mansoni* ameliorated the intestinal pathology associated with *T. gondii* infection by downregulating the IFN-γ and nitrous oxide typically associated with a Th1 response[24]. Unexpectedly, however, TNF-α levels were discordantly increased in the dually infected mice, resulting in severe liver pathology and premature death. Although this work supports our finding that enteric helminth infection can modulate the gastrointestinal inflammatory response, it also emphasizes that the eventual outcome in the infected host is dependent on the unique characteristics of the co-infecting parasites[24]. Parasitic third-stage larvae of *H. polygyrus* enter the wall of the anterior small intestine 24–72 hours after being ingested. After emerging into the lumen 9–11 days after infection, the larvae quickly mature into adults and establish a chronic infection in many mouse strains. Both experimental challenge infection (after worm clearance with antihelminthics) or repeated 'trickle' re-infection (to mimic the natural course of parasitic infection) elicit the vigorous Th2 response associated with protective immunity[25,26]. Adult worms in the upper duodenum, as well as the inflammatory lesions throughout the small intestine, localize this infection in close proximity to the *H. felis*-induced gastric immune response. Indeed, the local gastric cytokine and chemokine responses are altered more substantially by helminth co-infection than is the *H. felis*-specific serum antibody response. In contrast, in *S. mansoni* infection, female worms deposit eggs in the liver and gastrointestinal tract, resulting in more systemic pathologic changes.

Helicobacter-associated gastric cancer rates are lower in Africa than in countries like Peru and Colombia (the 'African enigma')[4]. However, widespread helminth infection is endemic throughout the Third World[27]. We have shown here that concurrent helminth infection can ameliorate helicobacter-induced gastric pathology, indicating involvement of Th2-biased parasitic infections in providing a possible explanation of this 'African enigma'. Furthermore, the influence of environmental variables such as altitude and rainfall on the prevalence of concurrent helminth infection may explain in part the differences in gastric cancer rates in different geographic locations with similar prevalence of *H. pylori* infection[28–33]. Thus, the epidemiology of specific types of helminth infections as well as the influence of diet, host genetic susceptibility, *H. pylori* genotype and other co-morbidity states in determining gastric cancer rates should be examined in these countries. Finally, the protective effect of concurrent helminth infection on the development of preneoplastic lesions such as gastric atrophy should be extended to studies on gastric cancer. The recently described helicobacter-dependent mouse model of gastric cancer, in which *H. felis*-induced inflammation leads rapidly to gastric atrophy and cancer (in less than 9 months) in hypergastrinemic transgenic mice, should prove suitable for these studies[22]. *H. polygyrus* is also ideal for this because this helminth sustains primary infection in C57/BL6 mice lasting several months[26].

Methods

Mice. Specific-pathogen-free, 6-week-old, female C57BL/6 mice (purchased from Jackson Labs, Bar Harbor, Maine) were used. Mice were maintained in facilities approved by the Association for Assessment and Accreditation of Laboratory Animal Care, and were housed in microisolator caging and provided rodent diet and water *ad libitum*. The mice were divided into four groups by treatment: uninfected (controls; $n = 5$); infected with *H. polygyrus* ($n = 5$); infected with *H. felis* ($n = 10$); and co-infected with *H. polygyrus* and *H. felis* ($n = 10$).

Experimental design. Infective, ensheathed third-stage larvae of the helminth parasite *H. polygyrus* were propagated as described[34] and stored at 4 °C. Infection with *H. polygyrus* used an 'antihelminthic-abbreviated immunizing protocol'[34]. On day 0, mice were inoculated orally with 200 third-stage larvae. On days 9 and 14 after infection, mice were treated orally with pyrantel pamoate (Apothecary Products. Minneapolis, Minnesota) at a dose of 172 mg/kg body weight, to eliminate adult parasites from the intestine. One week later (day 21), the mice were re-infected with 200 third-stage larvae. For infection with *H. felis*, mice were infected three times by mouth with about 10^8 colony-forming units of *H. felis* at an interval of every other day. For the co-infection group, this began on day 28 after infection with *H. polygyrus*.

The groups were then sub-divided, and one set of mice in each group was killed by CO_2 inhalation and examined 8 weeks after infection with *H.*

felis (or 12 weeks after infection with *H. polygyrus*). The second set of mice was analyzed 16 weeks after infection with *H. felis* (or 20 weeks after infection with *H. polygyrus*).

Sample preparation of sera and feces. Sera and feces were collected from all mice before they were given *H. felis*, and then every 2–4 weeks until necropsy. From each mouse, approximately 100 mg of freshly voided feces were suspended in a protease inhibitor 'cocktail' (1 μg/ml aprotonin, 10 μM leupeptin, 3.25 μM bestatin and 0.2 mM 4-(2-aminoethyl)-benzene sulfonylfluoride (all from Sigma), in 5% nonfat dry milk) as described[35]. The fecal slurry was microcentrifuged at 9330*g* for 10 min to yield supernatant for measurement of IgA.

Histopathologic evaluation. At 8 and 16 weeks after infection with *H. felis*, histopathologic evaluation of the gastric tissues was done as described[36]. A longitudinal strip from the greater curvature of the stomach, beginning at the squamocolumnar junction and ending at the gastroduodenal junction, was prepared from each mouse. Stomach tissues were fixed in neutral buffered 10% formalin, processed by standard methods, embedded in paraffin, cut into sections 5 μm in thickness, and stained with hematoxylin and eosin and Warthin-Starry argyrophilic silver stain. The glandular mucosa of the corpus and antrum were examined histologically for inflammatory and epithelial changes and for the presence of *H. felis*. Inflammation was distinguished histologically into chronic (lymphohistiocytic) and active (granulocytic) components. The contributions of each were graded on an ascending scale, from 0 to 4, based on the intensity, distribution and confluence of inflammatory infiltrates. Assessment of mucosal alterations was based on atrophy of glandular cells and epithelial hyperplasia; scores of 0–4 were assigned based on histologic estimation of the percentage of altered mucosa: 0, no substantial alteration; 1, less than 5%; 2, 25–50%; 3, 50–75%; and 4, more than 75%. Scores for bacterial colonization were assigned based on the relative frequency of colonized glands in the antral region using Warthin-Starry silver-stained sections, and discriminating sparsely colonized glands (score of 1 or 2) from those containing dense aggregates of bacteria (score of 3 or 4).

Enzyme-linked immunoassay (ELISA) for total serum IgG1 and IgE. The polyclonal, *H. polygyrus*-induced, serum IgG1 and IgE responses were detected by ELISA as described[37]. Immulon 2 plates (Dynax Technologies, Chantilly, Virginia) were coated with goat antibody against mouse IgG1 (Southern Biotechnology, Birmingham, Alabama) or rat antibody against mouse IgE (PharMingen, San Diego California). The blocked, washed plates were incubated for 1.5 h at room temperature with diluted serum samples in triplicate. IgG1 was detected with horseradish peroxidase-conjugated goat antibody against mouse IgG1 (Southern Biotechnology); IgE was detected with biotin-conjugated rat antibody against mouse IgE (PharMingen, San Diego, California) and peroxidase-conjugated streptavidin (Zymed Labs, San Francisco, California). Both reactions were developed with OPD (O-phenylenediamine dihydrochloride), and absorbance was measured at 492 nm. Absorbance values were converted to a measurement of μg/ml IgG1 and IgE by comparison with standard curves of purified IgG1 (Southern Biotechnology, Birmingham, Alabama) or IgE (PharMingen, San Diego, California) by linear regression analysis.

ELISA for antibodies against *H. felis* IgG, IgG1 and IgG2a in serum and IgA in feces. An outer-membrane antigen preparation of *H. felis* was obtained by methods that have been described[38]. *H. felis* was cultured for 48 h in micro-aerobic conditions in a trypticase soy broth containing 5% fetal bovine serum. After being washed three times in phosphate-buffered saline and examined for bacterial contaminants using Gram staining and phase microscopy, the pellet was resuspended for 30 min at room temperature in 4 ml 1% N-octyl-beta-glucopyranoside (Sigma). Insoluble material was removed by ultracentrifugation at 100,000*g* for 1 h. After dialysis against phosphate-buffered saline for 24 h at 4 °C, supernatant protein concentration was measured by the Lowry technique (Sigma).

For serum IgG measurement, 96-well plates were coated overnight at 4 °C with 100 μl per well of 1 μg/ml *H. felis* protein in carbonate buffer (pH 9.6). The coating concentration of antigen was increased to 10 μg/ml for subclass isotyping of the serum IgG response and measurement of IgA in fecal extracts. Serum was diluted 1:100 and fecal extracts were assayed undiluted. Biotinylated secondary antibodies included goat antibody against mouse IgG (Southern Biotechnology, Birmingham, Alabama), α-chain-specific goat antibody against mouse IgA (Sigma), and monoclonal rat antibodies produced by clones G1-6.5 and R19-15 (PharMingen, San Diego, California) for detecting mouse IgG1 and IgG2a, respectively. Incubation with extravidin peroxidase (Sigma) was followed by ABTS substrate (2,2'-azino-bis(3-ethylbenzothiazoline-6-sulfonic acid; Kirkegaard and Perry Laboratories, Gaithersburg, Maryland) for color development. Development of absorbance at a wavelength of 405 nm was recorded by an ELISA plate reader (Dynatech MR7000; Dynatech Laboratories, Chantilly, Virginia). Serum IgG, IgG1 and IgG2a results are reported as absorbance values at a sample dilution of 1:100. Because of an unknown dilution factor inherent in sample preparation, the absorbance measurement of IgA specific for *H. felis* in fecal extracts was standardized against total IgA concentration of the sample. A standard curve was generated on each ELISA plate by applying known amounts of purified mouse IgA-κ (Sigma) to wells precoated with α-chain-specific sheep antibody against mouse IgA.

RNA extraction and RT–PCR. Gastric mRNA was isolated from section of mouse stomach tissue 2 mm × 5 mm in size, containing both corpus and antrum. The tissue was immediately immersed in 2 ml Trizol® (Life Technologies) and 'snap-frozen'; RNA was then extracted following the manufacturer's directions. Reverse transcription (RT) was done as follows: 3 μg extracted RNA was added to reaction tubes containing 1 μl random hexamer primers (2.5 μg/μl; Boehringer), and RNAse-free H_2O was added to produce a total combined volume of 11 μl. The tubes were heated at 65 °C for 5 min and then placed on ice. Then, 9 μl master mix (4 μl 5x reaction buffer, 2 μl dNTP (10 mM), 1 μl DTT (100 mM), 1 μl rRNasin Rnase inhibitor and 1 μl M-MLV reverse transcriptase; all from Promega, Madison, Wisconsin) was added to each tube; this was heated for 55 min at 42 °C. For all PCR reactions, 1 μl RT product was used.

The following primers were used (forward and reverse): TGF-β, 5'–CGGGGCGACCTGGGCACCATCCATGAC 3' and 5'–CTGCTCCACCTTGGGCTTGCGACCCAC–3'; keratinocyte growth factor, 5'–TGGATACTGACACGGATCCTG–3' and 5'–GTCAATCCTCAGGTACCACT–3'; TNF-α, 5'–ATGAGCACAGAAAGCATGATC–3' and 5'–TACAGGCTTGTCACTCGAATT–3'; IL-1β, 5'–CAGGATGAGGACATGAGCACC–3' and 5'–CTCTGCAGACTCAAACTCCAC–3'; IL-10, 5'–GTGAAGACTTTCTTTCAAACAAAG–3' and 5'–CTGCTCCACTGCCTTGCTCTTATT–3'; IFN-γ, 5'–TACTGCCACGGCACAGTCATTGAA–3' and 5'–GCAGCGACTCCTTTTCCGCTTCCT–3'; IL-4, 5'–ACGGAGATGGATGTGCCAAACGTC–3' and 5'–CGAGTAATCCATTTGCATGATGC–3'; IL-5, 5'–GCCATGGAGATTCCCATGAGCACA–3' and 5'–GCCTTCCATTGCCCACTCTGTAC–3'; IL-6, 5'–CACAAAGCCAGAGTCCTTCAGAGA–3' and 5'–CTAGGTTTGCCGAGTAGATCTC–3'; IL-12(P35), 5'–CTTTGATGATGACCCTGTGC–3' and 5'–TTTGGGGAGATGAGATGTGA–3'; GAPDH, 5'–CGGAGTCAACGGATTTGGTCGTAT–3' and 5'–AGCCTTCTCCATGGTGGTGAAGAC–3'.

For these reactions, 1.5 mM $MgCl_2$ was used, except for IL-1β (1.0 mM) and IL-5 and IL-12 (p35) (2.0 mM). All cycle parameters, for a total of 30–40 cycles, were: 94 °C for 45 s, 60 °C for 45 s and 72 °C for 1.5 min, except for KGF (96 °C for 36 s, 56 °C for 1 min and 72 °C for 1.5 min), IL-10 (96 °C for 36 s'', 56 °C for 1 min and 72 °C for 1.5 min) and IL-12 (p35) (96 °C for 36 s, 55 °C for 1 min and 72 °C for 1.5 min). GAPDH primers were added to all reactions when 18–20 cycles remained.

Semi-quantitative PCR used the 'primer-dropping' method, in which GAPDH (glyceraldehyde phosphodehydrogenase) was co-amplified as an internal control in all reactions as described[39]. Aliquots of PCR reactions (approximately 30 μl) were equalized to the equivalent signals from the GAPDH mRNA and separated by electrophoresis through 2% agarose gels containing 0.2 μg/ml ethidium bromide. Gels were photographed and analyzed by densitometry using the National Institutes of Health Imaging software. Cytokine and growth factor mRNA levels of expression are presented as a ratio to GAPDH.

Chemokine RNA protection assay. Gastric chemokine mRNA expression was determined in mice co-infected with *H. polygyrus* and *H. felis* or infected with *H. felis* alone using a multi-template RNA protection assay (Riboquant®; PharMingen, San Diego, California) with the mCK-5 template set directed against lymphotactin, RANTES, eotaxin, MIP-1β, MIP-1α, MIP-2, IP-10, monocyte chemotactic peptide-1, T-cell activation 3 and internal controls of L32 (a ribosomal protein produced at steady-state levels); PharMingen,

San Diego, California) and GAPDH (PharMingen). The assay used 10 μg RNA, following the manufacturer's guidelines. The blot was exposed to film for 48 h to assess the chemokine regions and for 3 h to assess L32 and GAPDH. Relative expression levels were determined as described above and are expressed as a ratio of the expression of L32 and GAPDH.

Statistical analysis. Data for serum and fecal extract antibody, cytokine and chemokine responses are reported as a mean plus 1 standard error and were compared using the Students' *t*-test; $P < 0.05$ was considered statistically significant for differences between groups. Pathology data were compared using the Mann-Whitney analysis of nonparametric data.

Acknowledgments

We thank D. Podolsky and A. Luster for critical review of the manuscript. This work was supported by National Institutes of Health grants AI37740 (J.G.F.), CA67529 (J.G.F.) CA674463 (T.C.W. and J.G.F) and DK47017 (C.N.A.) and the Center for the Study of Inflammatory Bowel Disease at Massachusetts General Hospital (DK43351). H.N.S. was supported by a training fellowship from the Crohn's and Colitis Foundation of America.

RECEIVED 13 OCTOBER 1999; ACCEPTED 9 MARCH 2000

1. Graham, D.Y. *Helicobacter pylori* infection in the pathogenesis of duodenal ulcer and gastric cancer: a model. *Gastroenterology* **113**, 1983–1991 (1997).
2. Huang, J.-Q., Sridhar, S., Chen, Y. & Hunt, R.J. Meta-analysis of the relationship between *Helicobacter pylori* seropositivity and gastric cancer. *Gastroenterology* **114**, 1169–1179 (1998).
3. Ally, R., Mitchell, H.M. & Segal, I. cagA positive *H. pylori* aplenty in South Africa: the first systematic study of *H. pylori* infection in asymptomatic children in Soweto. *Gut* **45**, A97–98 (1999).
4. Holcombe, C. *Helicobacter pylori*: The African enigma. *Gut* **33**, 429–431 (1992).
5. Abbas, A.K., Murphy, K.M. & Sher, A. Functional diversity of helper T lymphocytes. *Nature* **383**, 787–793 (1996).
6. Mohammadi, M., Czinn, S., Redline, R. & Nedrud, J. Helicobacter-specific cell-mediated immune responses display a predominant Th1 phenotype and promote a delayed-type hypersensitive response in the stomachs of mice. *J. Immunol.* **156**, 4729–4738 (1996).
7. Bamford, K.B. *et al.* Lymphocytes in the human gastric mucosa during *Helicobacter pylori* have a T helper cell 1 phenotype. *Gastroenterology* **114**, 482–492 (1998).
8. Eaton, K.A., Ringler, S.R. & Danon, S.J. Murine splenocytes induce severe gastritis and delayed type hypersensitivity and suppress bacterial colonization in *Helicobacter pylori*-infected SCID mice. *Infect. Immun.* **67**, 4594–1602 (1999).
9. Roth, K.A., Kapadia, S.B., Martin, S.M. & Lorenz, R.G. Cellular immune responses are essential for the development of *Helicobacter felis*-associated gastric pathology. *J. Immunol.* **163**, 1490–1497 (1999).
10. Finkelman, F.D. *et al.* Cytokine regulation of host defense against parasitic gastrointesinal nematodes: lessons from studies with rodent models. *Annu. Rev. Immunol.* **15**, 505–533 (1997).
11. Sallusto, F., Mackay, C.R. & Lanzavecchia, A. Selective expression of the eotaxin receptor CCR3 by human T helper 2 cells. *Science* **277**, 2005–2007 (1997).
12. Bonecchi, R. *et al.* Differential expression of chemokine receptors and chemotactic responsiveness of Type 1 helper cells (Th1s) and Th2s. *J. Exp. Med.* **187**, 129–134 (1998).
13. Loetscher, P. *et al.* CCR5 is characteristic of Th1 lymphocytes. *Nature* **391**, 344–345 (1998).
14. Qin, S. *et al.* The chemokines receptors CXCR3 and CCR5 mark subsets of T cells associated with certain inflammatory reactions. *J. Clin. Invest.* **101**, 746–754 (1998).
15. Sawai, N. *et al.* Role of gamma interferon in *Helicobacter pylori*-induced gastric inflammatory responses in a mouse model. *Infect. Immun.* **67**, 279–285 (1999).
16. Sakagami, T. *et al.* Atrophic gastric changes in both *Helicobacter felis* and *Helicobacter pylori* infected mice are host dependent and separate from antral gastritis. *Gut* **39**, 639–648 (1996).
17. Taub, D.D. *et al.* Recombinant human interferon-inducible protein 10 is a chemoattractant for human monocytes and T lymphocytes and promotes T cell adhesion to endothelial cells. *J. Exp. Med.* **177**, 1809–1814 (1993).
18. Stellato, C. *et al.* Expression of the chemokine RANTES by a human bronchial epithelial cell line. Modulation by cytokines and glucocorticoids. *J. Immunol.* **155**, 410–418 (1995).
19. Zhou, Z.H. *et al.* IFN-γ induction of the human monocyte chemoattractant protein (hMCP)-1 gene in astrocytoma cells: functional interaction between an IFN-—activated site and a GC-rich element. *J. Immunol.* **160**, 3908–3916 (1998).
20. Fox, J.G. *et al.* Hypertrophic gastropathy in *Helicobacter felis* infected wildtype C57BL/6 mice and p53 hemizygous transgenic mice. *Gastroenterology* **110**, 155–166 (1996).
21. Berg, D.J., Lynch, N.A., Lynch, R.G. & Lauricella, D.M. Rapid development of severe hyperplastic gastritis with gastric epithelial dedifferentiation in *Helicobacter felis*-infected IL-$10^{-/-}$ mice. *Am. J. Pathol.* **152**, 1377–1386 (1998).
22. Wang, T. *et al.* Synergistic interaction between hypergastrinemia and Helicobacter infection in a mouse model of gastric carcinoma. *Gastroenterology* **118**, 36–47 (2000).
23. Goto, T. *et al.* Local secretory immunoglobulin A and post immunization gastritis correlate with protection against *Helicobacter pylori* infection after oral vaccination of mice. *Infect. Immun.* **67**, 2531–2539 (1999).
24. Marshall, A.J. *et al. Toxoplasma gondii* and *Schistosoma mansoni* synergize to promote hepatocyte dysfunction associated with high levels of plasma TNF-α and early death in C57BL/6 mice. *J. Immunol.* **163**, 2089–2097 (1999).
25. Behnke, J.M. & Brailsford, T.H. The dynamics of trickle infections with *Heligmosomoides polygyrus* in syngeneic strains of mice. *J Parasitol* **22**, 351–359 (1992).
26. Monroy, F.G. & Enriquez, F.J. *Heligmosomoides polygyrus*: A model for chronic gastrointestinal helminthiasis. *Parasitol. Today* **8**, 49–54 (1992).
27. Chan, M.S. The global burden of intestinal nematode infections-fifty years on. *Parasitol. Today* **13**, 438–443 (1997).
28. Barnish, G. & Ashford, R.W. *Stronglyloides cf. fuelleborni* and other intestinal helminths in Papua New Guinea: distribution according to environmental factors. *Parassitologia* **32**, 245–263 (1990).
29. Correa, P. *et al. Helicobacter pylori* and gastric carcinoma: serum antibody prevalence in populations with contrasting cancer risks. *Cancer* **66**, 2569–2574 (1990).
30. Schaap, H.B., Den Dulk, M.M.O. & Polderman, A.M. Schistosomiasis in the Yemen Arab Republic . Prevalence of *Schistosoma mansoni* and *S. haematobium* infection among schoolchildren in the central highlands and their relation to altitude. *Trop. Geogr. Med.* **44**, 19–22 (1992).
31. Genta, R.M., Gurer, I.E. & Graham, D.Y. Geographical pathology of *Helicoboacter pylori* infection: is there more than one gastritis? *Ann. Med.* **5**, 595–599 (1995).
32. Appleton, C.G. & Gouws, E. The distribution of common intestinal nematodes along an altitudinal transect in KwaZulu-Natal, South Africa. *Ann. Trop. Med. Parasitol.* **90**, 181–188 (1996).
33. Jemaneh, L. Comparative prevalences of some common intestinal helminth infections in different altitudinal regions in Ethiopia. *Ethiop. Med. J.* **36**, 1–8 (1998).
34. Shi, H.N., Scott, M.E., Koski, K.G., Boulay, M. & Stevenson, M.M. Energy restriction and severe zinc deficiency influence growth, survival and reproduction of *Heligmosomoides polygyrus* (Nematoda) during primary and challenge infections in mice. *Parasitology* **110**, 599–609 (1995).
35. Whary, M.T. *et al.* Chronic active hepatitis induced by *Helicobacter hepaticus* in the A/JCr mouse is associated with a Th1 cell-mediated immune response. *Infect. Immun.* **66**, 3142–3148 (1998).
36. Fox, J.G. *et al.* High salt diet induces gastric epithelial hyperplasia, parietal cell loss, and enhances *Helicobacter pylori* colonization in C57BL/6 mice. *Cancer Res.* **59**, 4823–4828 (1999).
37. Shi, H.N., Ingui, C.J., Dodge, I. & Nagler-Anderson, C. A helminth-induced mucosal Th2 response alters nonresponsiveness to oral administration of a soluble antigen. *J. Immunol.* **160**, 2449–2455 (1998).
38. Pronovost, A.D., Rose, S.L., Pawlak, W., Robin, H. & Schneider, R. Evaluation of a new immunodiagnostic assay for *Helicobacter pylori* antibody detection: correlation with histopathological and microbiological results. *J. Clin. Microbiol.* **32**, 46–50 (1994).
39. Wong, H., Anderson, W.D., Cheng, T. & Riabowol, K.T. Monitoring mRNA expression by polymerase chain reaction: the "primer dropping" method. *Analytical Biochem.* **223**, 251–258 (1994).